CI&CEQ

Available on line at
Association of the Chemical Engineers of Serbia AChE
www.ache.org.rs/CICEQ

Chemical Industry & Chemical Engineering Quarterly 19 (2) 195–212 (2013) CI&CEQ

S. SURESH[1]
V.C. SRIVASTAVA[2]
I.M. MISHRA[2]

[1]Department of Chemical Engineering, Maulana Azad National Institute of Technology Bhopal, Bhopal, India
[2]Department of Chemical Engineering, Indian Institute of Technology Roorkee, Roorkee, India

SCIENTIFIC PAPER

UDC 66.09:547.562:547.551.1:66.081.5

DOI 10.2298/CICEQ111225054S

STUDIES OF ADSORPTION KINETICS AND REGENERATION OF ANILINE, PHENOL, 4-CHLOROPHENOL AND 4-NITROPHENOL BY ACTIVATED CARBON

The present paper reports kinetic studies of the adsorption of aniline (AN), phenol (P), 4-chlorophenol (CP) and 4-nitrophenol (NP) from aqueous solution onto granular activated carbon (GAC). In FTIR spectral analysis, the transmittance of the peaks gets increased after the loading of AN, P, CP and NP signifying the participation of these functional groups in the adsorption and it seems that the adsorption of AN, P, CP and NP is chemisorptive in nature. The rates of adsorption were found to obey a pseudo-second order model and that the dynamics of AN, P, CP and NP adsorption are controlled by a combination of surface and pore diffusion. The diffusion coefficients were of the order of 10^{-10} m^2 s^{-1}. Thermal desorption at 623 K was found to be more effective than solvent desorption. GAC performed well for at least five adsorption-desorption cycles, with continuous decrease in adsorption efficiency after each thermal desorption. Owing to its relative high heating value, the spent GAC can be used as a co-fuel for the production of heat in a boiler or a furnace.

Keywords: GAC, aniline, phenols, kinetics, pseudo-first-order, pseudo-second-order, desorption, solvent, thermal.

Phenol (P) and its derivatives are ionizable organic compounds that are regarded as environmentally relevant contaminants. They are widely fo-und in pesticides, dyestuffs, pharmaceuticals, oil refineries, coke plants, plastic industry, petrochemicals, and other industrial effluents [1-4]. Phenols (Ps) are also used in the manufacture of P-formaldehyde resins for surface coatings and as bonding agents in laminated products, among other uses. Chlorophenols (CPs) and nitrophenols (NPs) are used as pesticides, bactericides, wood preservatives and synthetic intermediates [5]. CPs are typical byproducts of the chlorine bleaching process used in pulp and paper mills. NPs are among the most common organic pollutants in industrial and agricultural wastewater. These compounds are involved in the synthesis of many chemicals, particularly in the field of pesticides. Aniline (AN) has been found to distribute in an aqueous environment and causes teratosis in aquatic species [5]. It is known to be carcinogenic [6]. It reacts easily in the blood to convert hemoglobin into methahemoglobin, thereby preventing oxygen uptake [7]. Ps and their substituted compounds are thus important environmental pollutants [8-12]. The USEPA recommends a maximum level of 1 μg mL^{-1} of total phenolic compounds in water supplies [12]. Adsorption processes using GAC are widely employed for the removal of trace organic contaminants such as P, AN and its derivatives from drinking waters and industrial effluents.

Conventional methods for the removal of Ps and AN from wastewaters include solvent extraction, biodegradation [13-14], catalytic oxidation [15], membrane separation [16-17], ultrasonic degradation [18], supercritical water oxidation [19], and electrochemical oxidation [20], photodegradation [21], flocculation [22], chemical oxidation [23-25], as well as biological process [6,26]. Many workers have reported on the adsorptive removal of AN [3,27-28] and Ps [29-31] from aqueous solutions. The adsorption of P and substituted Ps from aqueous solution on activated car-

Correspondence: S. Suresh, Department of Chemical Engineering, Maulana Azad National Institute of Technology Bhopal, Bhopal-462 051, India.
E-mail: sureshpecchem@gmail.com
Paper received: 25 December, 2011
Paper revised: 13 March, 2012
Paper accepted: 30 May, 2012

bons (ACs) has also been extensively investigated [31-36].

In the present study we determine the GAC characteristics from SEM, FTIR and TGA analyses and also report the effects the initial pH (pH_0), adsorbent dose (m), initial concentration (C_0) and contact time (t) on the adsorption efficiency. The kinetics of adsorption were studied and various kinetic models were tested against experimental data in an effort to gain insight into the adsorption and desorption mechanisms.

MATERIALS AND METHODS

GAC and its characterization

The GAC used in the present study was procured from S.D. Fine Chemicals Limited, Mumbai, India. The average particle size was calculated to be 1.671 mm. Proximate analysis showed the presence of 9.04% moisture, 12.70% volatile matter and 78.87% fixed carbon in blank-GAC. No ash was found in the blank. The BET surface area of GAC was 977.05 m^2 g^{-1}, whereas the BJH adsorption/desorption surface area of pores was 45.03/47.63 m^2 g^{-1}. The single point total pore volume of pores was found to be 0.4595 cm^3 g^{-1}, whereas the cumulative adsorption and desorption volumes of the pores (17 Å < d < < 3000 Å) were 0.0717 and 0.0789 cm^3 g^{-1}, respectively. The BET average pore diameter of GAC was found to be 18.79 Å. The bulk density and heating value of GAC were found to be 725 kg m^{-3} and 8.51 MJ kg^{-1}, respectively.

Chemicals

All the chemicals used in the study were of analytical reagent (AR) grade. AN ($C_6H_5NH_2$; CAS No.62--53-3) was procured from Qualigens Fine Chemicals, Mumbai, India. P (C_6H_5OH; CAS No.108-95-2) was procured from Ranbaxy Fine Chemicals, New Delhi, India. CP (4-ClC_6H_4OH; CAS No.106-48-9), NP (4-$NO_2C_6H_5OH$; CAS No. 10-02-7), NaOH, and HCl were obtained from S.D. Fine Chemicals, Mumbai, India. Stock solutions of AN, P, CP and NP were made by dissolving exact amount of AN, P, CP and NP in distilled water, respectively. These test solutions were prepared by diluting 1 g dm^{-3} of stock solution of AN, P, CP and NP with double-distilled water.

Analysis of AN, P, CP and NP

The initial and residual concentration of AN, P, CP and NP were determined by finding the absorbance of the respective solution at 230, 269, 279 and 317 nm, respectively, using a UV/Vis spectrophotometer (Lambada 35; PerkinElmer, MA 02451, USA). First, calibration plots of absorbance *versus* concentration were made after all adsorbates. The calibration plots of AN, P, CP and NP showed a linear variation up to concentrations of 0.27, 1.06, 0.78 and 0.36 mmol dm^{-3}, respectively. Before the analysis, the samples were diluted to concentrations in the linear range, whenever necessary, with double-distilled water.

Batch adsorption programme

For each experimental run, 100 ml aqueous solution of known concentration of AN, P, CP and NP was taken in a 250 ml conical flask containing a known mass of GAC. In all the experimented, the pH of the solution was maintained constant using buffer system of potassium dihydrogen orthophosphate (KH_2PO_4) and sodium hydroxide (NaOH). These flasks were agitated at a constant shaking rate of 150 rpm in a temperature controlled orbital shaker (Metrex Scientific Instruments, New Delhi) maintained at 303 K. To determine the adsorption kinetics, the samples were withdrawn at different time intervals up to 24 h, centrifuged using a Research Centrifuge (Remi Instruments, Mumbai) at 10000 rpm for 5 min, after which the supernatant liquid was analyzed for residual concentrations of AN, P, CP and NP. The removal of AN, P, CP and NP from the solution and the adsorption uptake in solid phase (q_t) were calculated using the following relationships:

Percentage of AN or P or CP or NP removal =
$$= 100(C_0 - C_t)/C_0 \quad (1)$$

Amount of adsorbed AN or P or CP or NP per g of solid:

$$q_t = (C_0 - C_t)V/m \quad (2)$$

where C_0 is the initial AN, P, CP and NP concentration (mmol dm^{-3}), C_t is the AN, P, CP and NP concentration (mmol dm^{-3}) at any time t, V is the volume of the solution (dm^3) and m is the mass of the adsorbent (g). For equilibrium values, the corresponding values at equilibrium time were taken for calculation.

Adsorption kinetic theory

Diffusion study

The possibility of intra-particle diffusion was explored by using the intra-particle diffusion model [37] given by following equation:

$$q_t = k_{id} t^{1/2} + I \quad (3)$$

where k_{id} is the intra-particle diffusion rate constant, and values of I give an idea about the thickness of the boundary layer. In order to check whether surface dif-

fusion controlled the adsorption process, the kinetic data were further analyzed using the Boyd kinetic expression, which is given by [38-39]:

$$F = 1 - \frac{6}{\pi^2}\exp(-B_t) \text{ or } B_t = -0.4977 - \ln(1-F) \quad (4)$$

where $F(t) = q_t/q_e$ is the fractional attainment of equilibrium at time t, and B_t is a mathematical function of F.

Kinetic data were further treated by models given by Boyd *et al.* [38] and simplified by applying a solution given by the Skelland and Vermeules approximation [39-40] for calculating effective diffusivity:

$$\ln\left[\frac{1}{(1-F^2(t))}\right] = \frac{\pi^2 D_e t}{R_a^2} \quad (5)$$

where D_e is the effective diffusion coefficient of adsorbates in the adsorbent phase ($m^2\ s^{-1}$), R_a is the radius of the adsorbent particle assumed to be spherical (m). The slope of the plot of $\ln\left[1/(1-F^2(t)\right]$ *vs.* t gives D_e.

Pseudo-first-order- and pseudo-second-order-model

The adsorption of AN, P, CP and NP molecules from the liquid phase to the solid phase can be considered as a reversible process with equilibrium being established between the solution and the solid phase. Assuming non-dissociating molecular adsorption of AN, P, CP and NP molecules on GAC particles with no AN, P, CP and NP molecules initially present on the adsorbent, the uptake of the AN, P, CP and NP molecules by the GAC at any instant t is given as [31]:

$$q_t = q_e\left[1 - \exp\left(-k_f t\right)\right] \quad (6)$$

where q_e is the amount of the adsorbate adsorbed on the adsorbent under equilibrium condition and k_f is the pseudo-first-order rate constant. The pseudo-second-order model is represented as [41]:

$$q_t = \frac{tk_S q_e^2}{1 + tk_S q_e} \quad (7)$$

The initial adsorption rate, h (mg g^{-1} min^{-1}), at $t \to 0$ is defined as:

$$h = k_S q_e^2 \quad (8)$$

The Marquardt's percent standard deviation (MPSD) error function [42] was employed in this study to find out the most suitable kinetic model to represent the experimental data. This error function is given as:

$$MPSD = 100\sqrt{\frac{1}{n_m - n_p}\sum_{i=1}^{n}\left(\frac{q_{e,i,\exp} - q_{e,i,\text{cal}}}{q_{e,i,\exp}}\right)^2} \quad (9)$$

In this equation, the subscript exp and calc represent the experimental and calculated values, n_m is the number of measurements, and n_p is the number of parameters in the model.

RESULTS AND DISCUSSION

GAC and its characterization

The SEM micrographs for blank GAC are shown in Figure 1. The GAC shows random type of pores with cracks and crevices. Similar micrographs were obtained for AN, P, CP and NP-loaded GAC (not shown here). At low magnification, the surface texture of blank and AN, P, CP and NP-loaded GAC were found to be similar with very little difference. However, at high magnification, AN, P, CP and NP-loaded GAC showed bright spots which may be due to the pore filling by AN, P, CP and NP. EDX analysis (Table 1) shows the GAC to be mainly carbonaceous with 90.4% carbon, 9% oxygen, and 0.6% other.

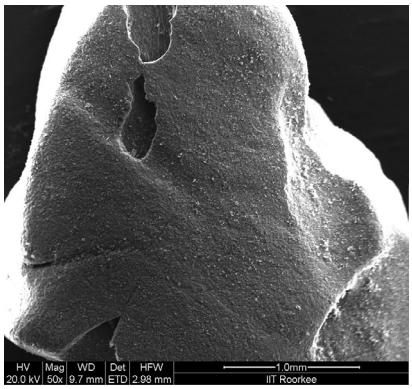

50×

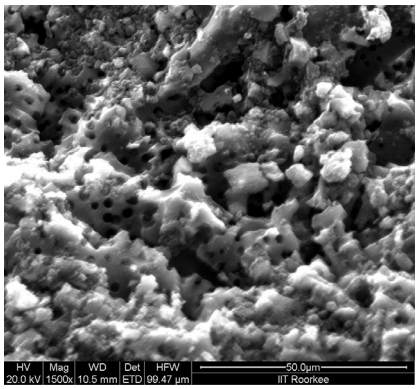

1500×

Figure 1. SEM of virgin-GAC.

The nature of interaction between AN, P, CP and NP molecules and ions with functional groups present on the GAC surface was assessed through FTIR spectral analysis. The infrared spectra of GAC,

Table 1. Physico-chemical characteristics of GAC and loaded-GAC

Characteristics	GAC	AN-GAC	P-GAC	CP-GAC	NP-GAC
Proximate analysis					
Moisture (%)	9.04	1.62	1.34	1.72	1.24
Volatile matter (%)	12.09	10.54	12.18	11.17	10.71
Fixed Carbon (%)	78.87	87.84	86.48	87.11	88.05
Bulk density (kg m^{-3})	725	-	-	-	-
Heating value (MJ kg^{-1})	8.26	14.3	8.89	9.84	10.45
Average particle size (mm)	3.161	-	-	-	-
EDX Analysis					
C (%)	90.41	88.28	91.08	92.14	89.67
O (%)	9.01	6.30	7.28	4.08	3.89
N (%)	-	3.85	-	-	2.96
Cl (%)	-	-	-	3.18	-
Al (%)	0.15	0.52	0.55	0.13	0.44
Mg(%)	0.26	0.35	0.44	0.2	0.58
Surface area of pores, m^2 g^{-1}					
(i) BET	977	-	-	-	-
(ii) BJH					
(a) adsorption cumulative	45	-	-	-	-
(b) desorption cumulative	48	-	-	-	-
BJH cumulative pore volume, cm^3 g^{-1}					
(i) Single point total	0.4595[a]	-	-	-	-
(ii) BJH adsorption	0.0717[b]	-	-	-	-
(iii) BJH desorption	0.0789[b]	-	-	-	-
Average pore diameter (Å)		-	-	-	-
(i) BET	19	-	-	-	-
(ii) BJH adsorption	63[b]	-	-	-	-
(iii) BJH desorption	66[b]	-	-	-	-
pH_{PZC}	10.3	-	-	-	-

[a]Pores less than 5666 Å; [b]pores diameter between 17 and 3000 Å

AN, P, CP, NP and AN-, P-, CP- and NP-GAC are shown in Figures 2-4. Blank-GAC (Figure 2) shows a broad band with centre at 3450 cm^{-1} indicative of the presence of both free and hydrogen bonded OH groups on the GAC surface. The FTIR spectrum of blank GAC shows a weak and broad peak in the region of 1620 cm^{-1}. The broad peak in the region of 1602 cm^{-1} indicates the presence of CO group stretching from aldehydes and ketones. The band at 1600 cm^{-1} may also be due to conjugated hydrocarbon bonded carbonyl groups. The FTIR spectra also show transmittance around 1115 cm^{-1} region due to the vibration of the CC group in lactones and due to -COH stretching and -OH deformation.

Figure 3a shows that the pure and loaded-GAC spectrum of AN. The spectrum of AN can be assigned as: a band at 3347.95 cm^{-1} for stretching vibration of $-NH_2$ group; a ring stretching with a contribution of the NH_2 scissoring band at 1610.96 cm^{-1}. The mode at 1276.71 cm^{-1} is assigned as partly to C-N stretching and partly to the ring stretching vibration [43-44]. Figure 3b shows the FTIR spectra of pure AN and after AN adsorption onto GAC. The peak at 3331.51 cm^{-1} and 3041.10 cm^{-1} were assigned to OH stretching and aromatic C-H stretching. The peaks at 1468.49, 1364.38, 805.48 and 690.41 cm^{-1} were diminished, while the absorbance band of hydroxymethyl and methylene groups increased. The peaks at 1468.49 cm^{-1} corresponded to the C=C aromatic ring vibrations. The peaks at 1364.38 cm^{-1} corresponded to the C-H bending in plane, while the 690.41 cm^{-1} peaks belonged to the C-H out of plane vibrations. Similar peaks were observed by [45-46].

Strong band at 1589.82 and 1489.02 cm^{-1} in the spectrum of pure CP (Figure 4a) can be attributed to C=C stretching. This band was observed as 1590 cm^{-1} by other researcher for the interaction between activated carbon surfaces and adsorbed P derivatives [47].

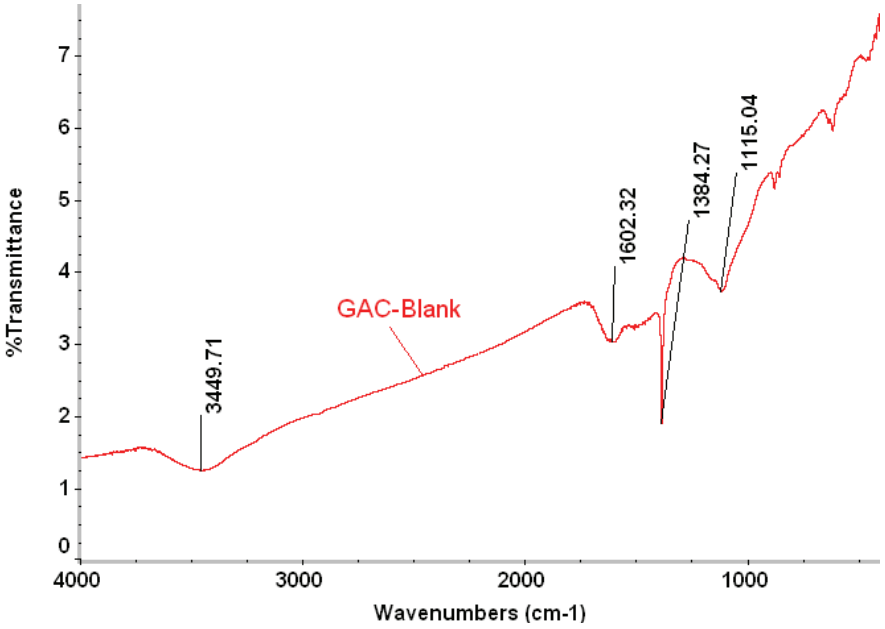

Figure 2. FTIR of virgin-GAC.

The band at 1369.86 cm^{-1} was attributed to the in-plane bending of C-H bonds. The band at 1090.36 cm^{-1} is assigned to a C-Cl vibration. The band at 810.96 cm^{-1} was attributed to mostly out-of-plane bending of the ring C-H vibration. Similar peaks were observed by previous investigators [46,48-49].

Figure 4b shows the FTIR spectra of NP loaded GAC. Bands appearing at 3429 and 2966.52 cm^{-1} were assigned to OH stretching and C-H stretching of aromatic. The variations in intensity of the bands at 3421.38 and 3084.93 cm^{-1} shows the adsorption of NP. The bands at 1923.29, 1614.28, 750.68 and 629.16 cm^{-1} were due to C≡C stretching, C≡O stretching of carboxylic group, methylene rocking band and ≡C-H bending mode, respectively. Out of these, carboxylic and hydroxyl groups played a major role in the removal of NP. Bands at 1499.42 and 1384.38 cm^{-1} were typical of NO_2 group indicating the adsorption of NP. The presence of a medium peak at 750.68 cm^{-1} further confirmed the adsorption of para-substituted benzene product. Similar peaks were observed by [50].

It may be seen that few peak appear in AN, P, CP and NP loaded GAC and few of the peaks originally present in GAC get shifted. Also the transmittance of the peaks gets increased after the loading of AN, P, CP and NP signifying the participation of these functional groups in the adsorption and it seems that the adsorption of AN, P, CP and NP is chemisorptive in nature.

Effect of initial pH (pH_0)

At low pH (*e.g.*, pH < point of zero charge (pH_{pzc})), most ACs are positively charged, at least in part as a consequence of donor/acceptor interactions between the carbon graphene layers and the hydronium ions [51]. The pH_{pzc} for GAC used in the present study lies at the pH_0 value of 10.3 (not shown here).

For a solution containing P and having pH > pH_{pzc} of P, mainly phenolate anions are formed. It can be presumed that in the case of P adsorption, the positive surface charge resulting from the adsorption of protons by the strongest surface bases still attracts water and ionic species, thus blocking some active sites and preventing complete pore filling by P [52] and also electrostatic repulsion phenomenon was produced which the lower amount adsorbed at acidic pH [53-55].

The pK_a values of AN, P, CP and NP were 4.63, 9.95, 9.38 and 7.15, respectively [56-57]. AN, P, CP and NP species are found to be present in deionized water in the form of AN, P, CP and NP. For AN, the ratio of $C_6H_5NH_2$ to $C_6H_5NH_3^+$ ≈99% at pH 7; for P, the ratio of C_6H_5OH to $C_6H_5O^-$ is ≈0.99 at pH 6; for CP, the ratio of C_6H_4ClOH to $C_6H_4ClO^-$ is ≈0.99 at pH 5.75; and for NP, the ratio of $C_6H_4(NO_2)OH$ to $C_6H_4(NO_2)O^-$ is ≈93.3 at pH 6. The concentration of the hydrolyzed AN, P, CP and NP species depends on the total AN, P, CP and NP concentrations and the solution pH. The speciation of AN, P, CP and NP in deionized water is presented in Figure 5. The percentage of AN, P, CP and NP hydrolytic products was calculated from the following stability constants.

The effect of pH_0 on the adsorption of AN, P, CP and NP (C_0 = 1.07, 1.06, 0.78 and 0.72 mmol dm^{-3}, respectively) onto GAC was studied at a temperature

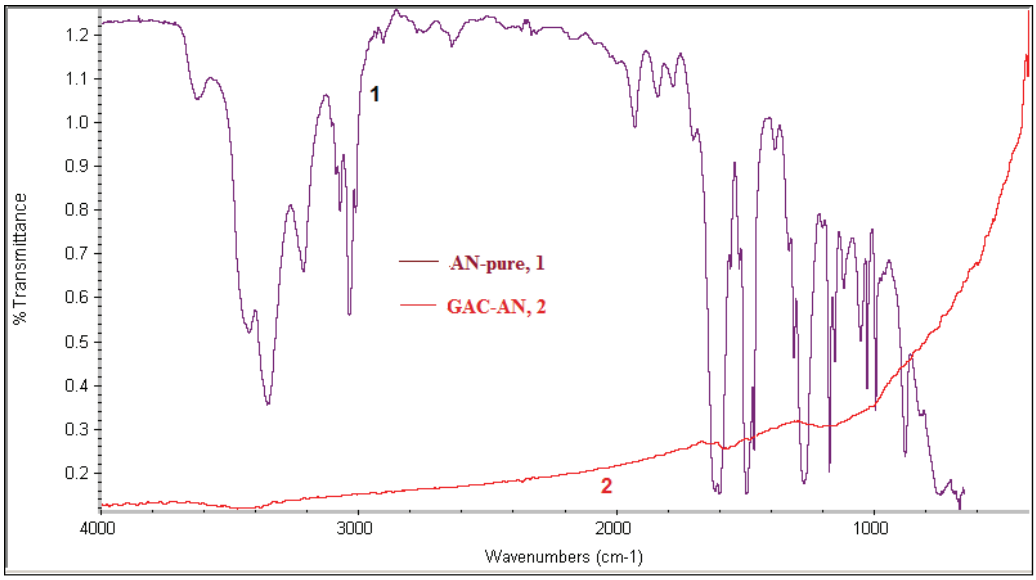

(a)

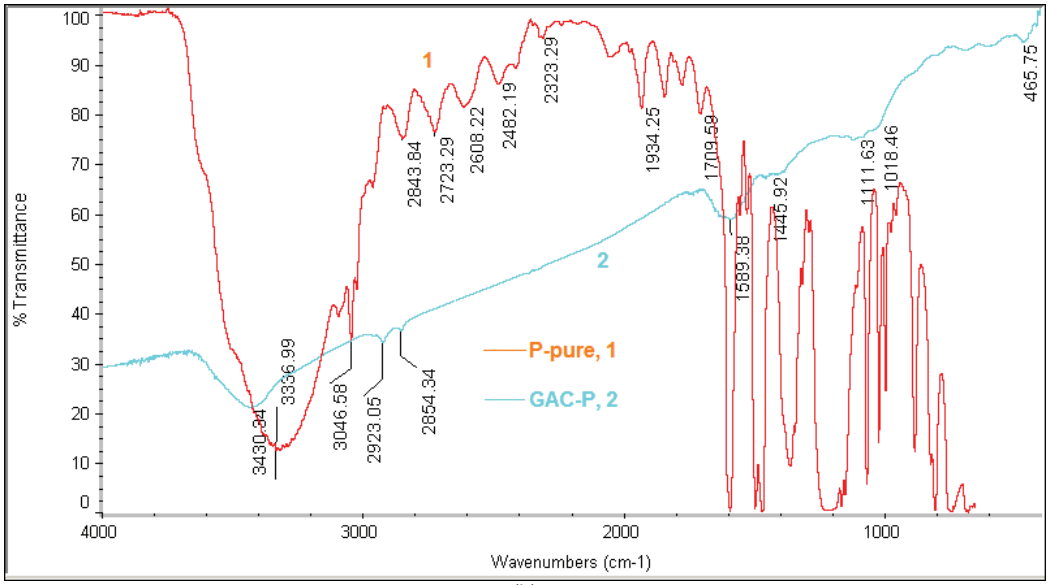

(b)

Figure 3. FTIR of AN, P and AN, P loaded GAC; a) 1: pure AN; 2: AN-GAC; b) 1: pure P; 2: P-GAC.

of 303 K by varying the pH_0 in the range of 2-12. Natural pH of AN, P, CP and NP solution at C_0 =1.07, 1.06, 0.78 and 0.72 were 6.9, 6, 5.75 and 6, respectively. The results of the experiments are presented in Figure 6. It can be seen that the removal of the AN, P, CP and NP slightly increased with an increase in pH_0 of the solution from 2 to natural pH. Further increase in pH_0 from natural pH to 12 led to a sharp decrease in the AN, P, CP and NP removal efficiency. Zheng *et al*. [58] found that the adsorption efficiencies of AN onto Cr-bentonite are high and stable under acidic and neutral pH conditions and decrease with the increase of pH value under alkaline pH conditions. Lower sorption of AN at alkaline pH is probably due to the presence of excess OH^- competing with AN for hydrogen bond formed with water molecules coordinated with chromium ion in interlayer [58]. The percentage adsorption were found to be close to 97, 94.3, 97.4 and 87.62% for AN, P, CP and NP, respectively, at pH_0 4; and 99.3, 98.2, 98.7 and 94.8%, respectively at natural pH. Percentage adsorption decreased sharply for $pH_0 \geq 6$ for AN, P, CP and NP. However, decrease in removal efficiency for NP and CP was much sharper than as compared to that for AN and P.

The main contributions to organics adsorption onto GAC are π-π dispersion interactions [59], hydrogen-bonding interactions [60] and donor-acceptor

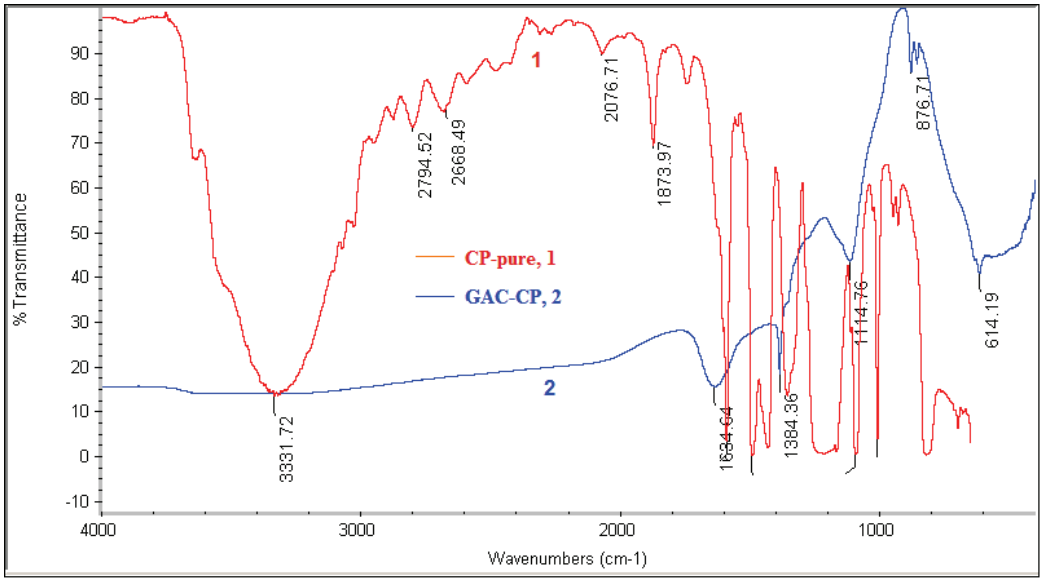

(a)

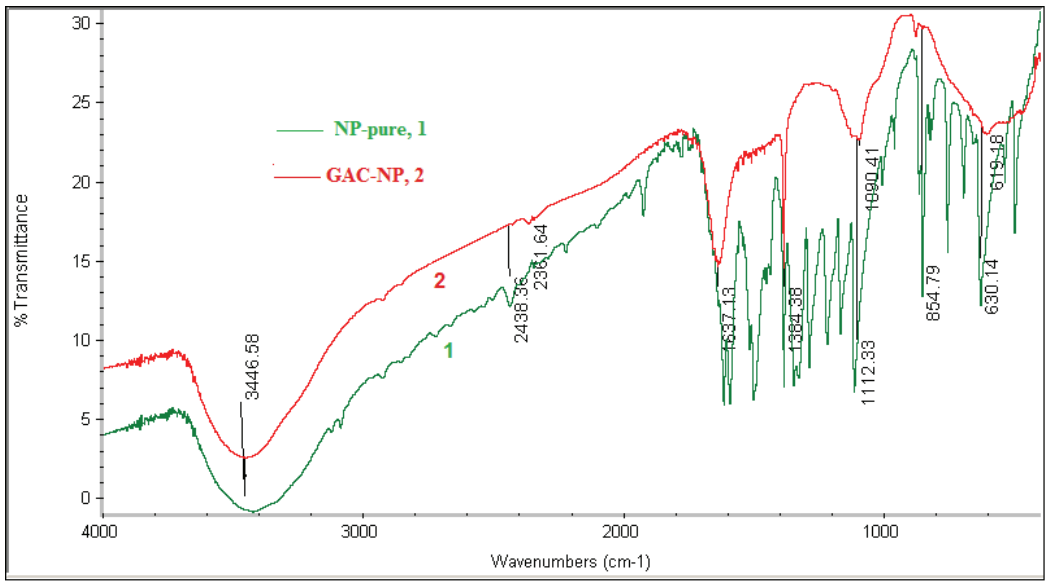

(b)

Figure 4. FTIR of CP, NP and CP, NP loaded GAC; a) 1: pure CP; 2: CP-GAC; b) 1: pure NP; 2: NP-GAC.

interactions [61]. The substituents on benzene ring provide different inductive and resonance effects, and their relative electron donating properties are well-known [62]. Hydroxyl is an electron-donating functional group [63] which can increase the π-donating strength of the host aromatic ring. Thus, -OH can increase the adsorption affinity of the phenolic compounds to the GAC graphene surfaces [64]. It is obvious that π-π dispersive interactions will be stronger with the increase of the number of hydroxyl. Therefore, the number of hydroxyl has positive effect on the adsorption of phenolic derivatives. Previous investigators have shown that the substitution of P with a hydroxyl in *meta*-position results in a much higher adsorption amount than substitution in the *ortho*- and *para*-position [65].

The increased surface acidity of GAC at pH ≈6 favors the donor-acceptor interaction between the electrons of the aromatic ring and the surface. This leads to an increase of the removal efficiency [65]. However, the increasing removal efficiency of AN, P, CP and NP by GAC within pH 2-6 suggests the insignificant involvement of hydrogen bonding between the phenolic and GAC [66]. Increasing adsorption of these polar aromatics to GAC with increasing pH before their pK_a may be due to the change of GAC properties with pH. At pH ≤ pH_{pzc}, the GAC surface is positively charged and the species adsorbed at pH (7,

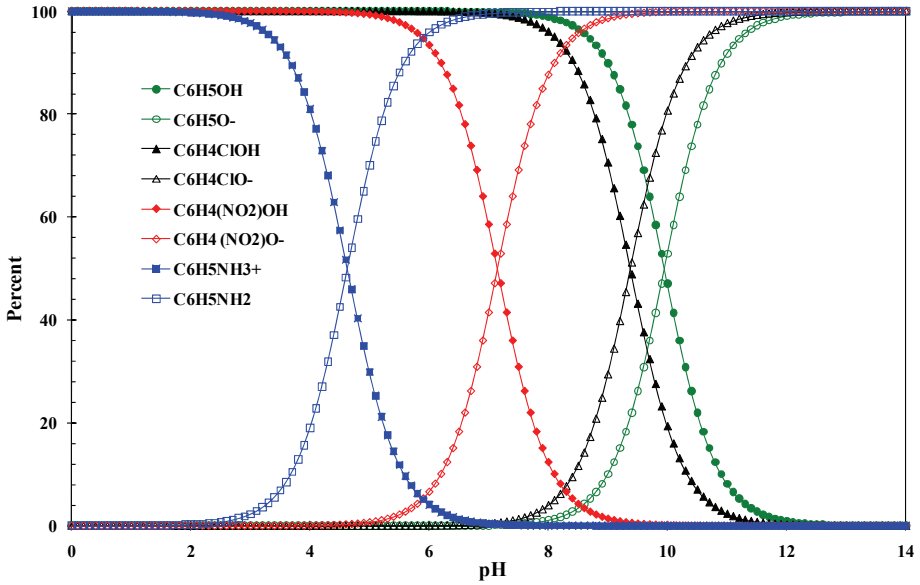

Figure 5. Distribution of AN, P, CP and NP as a function of pH.

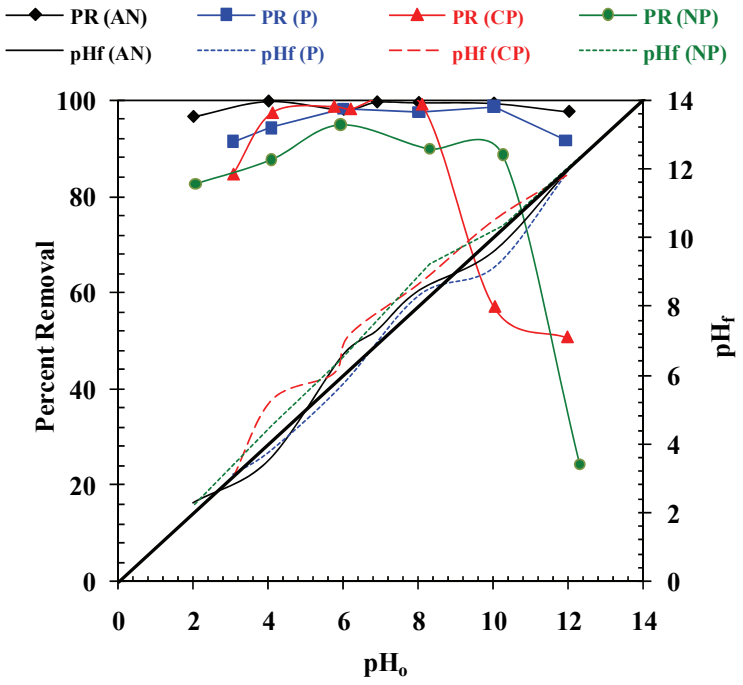

Figure 6. Effect of pH_0 on the adsorption of AN, P, CP andNP by GAC. T = 303 K, t = 24 h, C_0 = 100 mg dm^{-3}, GAC dose = 10 g dm^{-3}.

6 and 5.75) are neutral molecules that were adsorbed significantly due to the dispersive or van der Waals interactions determining the adsorption process [65,67].

Effect of GAC dosage (*m*)

Figure 7 shows the AN, P, CP and NP removal efficiency as a function of GAC dosage with C_0 of 1.07, 1.06, 0.78 and 0.72 mmol dm^{-3}, respectively, and t = 24 h. The AN, P, CP and NP removal efficiency increased from 29.2, 38.3, 23.4 and 47.07% at m = 1 g dm^{-3} to 86.47, 90.74, 96.69 and 87.8%, respectively, at m = 5 g dm^{-3}. For $m \geq$ 10 g dm^{-3}, AN, P, CP and NP removal efficiencies became constant at 95.8, 97.3, 98.56 and 98.4%, respectively. The increase in adsorption of AN, P, CP and NP with an increase in m up to 10 g dm^{-3} was due the presence of a greater number of adsorbent sites at increased m. The adsorption efficiency of AN and CP increases with the increase of adsorbent dosage upto 10 g dm^{-3} and remain almost constant onto XAD-4 and Cr-bentonite [68-69]. Similar results were reported for 4-hydroxyphenol sorption on Cr-bentonite from aqueous solu-

tion [69]. However, for $m \geq 10$ g dm^{-3}, the AN, P, CP and NP removal efficiencies become less dependent on m. Varying amounts of AC were contacted with the BSM containing 1000 mg dm^{-3} of P or NP to optimize the dose of adsorbent. Kumar *et al.* [70] reported that NP showed more adsorbability than P. Only 6 g dm^{-3} of AC dose was required in case of NP as against the 10 g dm^{-3} of AC dose to effect the same amount of P, *i.e.*, 95%, showing a good interaction between the nitro-group of NP and functional groups present on the AC surface. After 95% removal, the AC dose is not very effective, suggesting that the whole of the P and NP concentration cannot be reduced efficiently to zero in a single stage batch reactor.

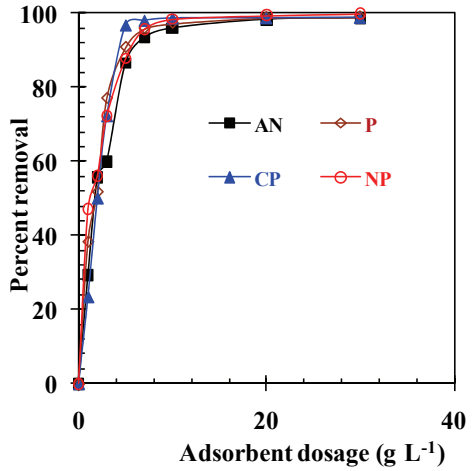

Figure 7. Effect of adsorbent dose on the adsorption of AN, P, CP and NP by GAC. T = 303 K, t = 24 h, C_0 = 500 mg dm^{-3}.

Effect of contact time and initial AN, P, CP and NP concentration

The effect of contact time on the q_t values for C_0 0.54-10.74 mmol dm^{-3}, 0.21-10.62 mmol dm^{-3}, 0.15-7.78 mmol dm^{-3} and 0.14-7.19 mmol dm^{-3} for AN, P, CP and NP at m = 10 g dm^{-3} and T = 303 K is shown in Figures 8a-8d. The adsorption was followed over a period of 24 h. These durations are considered to be approximately the equilibration times for the adsorption process. It may be seen that in the first 1 h, brisk adsorption of AN, P, CP and NP occurred at all C_0 and, thereafter, the adsorption rate decreased gradually and the adsorption reached equilibrium. For $C_0 \leq$ ≤ 2.68, 2.66, 1.94 and 1.80 mmol dm^{-3} the residual concentrations at 5 h contact time were found to be higher by a maximum of around 2% than those obtained after 24 h contact time for AN, P, CP and NP, respectively. Therefore, after 5 h contact time, a steady state approximation was assumed and a quasi-equilibrium situation was accepted for $C_0 \leq 2.68$ mmol dm^{-3}. For AN adsorption onto GAC, equilibrium adsorption time were found to be 5 (96.5%), 5 (97.7%), 8 (97.8%), 16 (98.6%) and 20 h (92.4%) respectively, at C_0 values of 0.54, 1.07, 2.68, 5.37 and 10.74 mmol/l. For P adsorption onto GAC, equilibrium adsorption time were found to be 5 (97.2%), 5 (97.3%), 8 (97.2%), 5 (98.6%) and 5 h (99.2%) respectively, at C_0 values of 0.53, 1.06, 2.66, 5.31 and 10.63 mmol dm^{-3}, For CP adsorption onto GAC, equilibrium adsorption time were found to be 2 (97.9%), 3 (98.5%), 5 (98.3%), 5 (99.5%) and 3 h (99.1%) respectively, at C_0 values of 0.39, 0.78, 1.94, 3.89 and 7.78 mmol dm^{-3} and For NP adsorption onto GAC, equilibrium adsorption time were found to be 3 (98.1%), 5 (96.5%), 5 (97.5%), 8 (95.6%) and 12 h (94.1%) respectively, at C_0 values of 0.36, 0.72, 1.80, 3.59 and 7.19 mmol L^{-1}. The rate of AN, P, CP and NP removal by GAC is fast for the first 1 h. This is obvious from the fact that a large number of vacant surface sites are available for the adsorption during the initial stage and with the passage of time, the remaining vacant surface sites were difficult to be occupied due to repulsive forces between the solute molecules on the solid phase and in the bulk liquid phase. Also, the adsorbates get adsorbed into the mesopores of GAC that get almost saturated during the initial stage of adsorption. Thereafter, the adsorbates have to traverse farther and deeper into the pores encountering much larger resistance. This results in the slowing down of the adsorption during the later period of adsorption.

Various researchers have reported that C_0 provides an important driving force to overcome all mass transfer resistances of the adsorbates between the aqueous and solid phases. The increase in C_0 also enhances the interaction between adsorbate molecules and the vacant sorption sites on the GAC and the surface functional groups. Therefore, an increase in C_0 enhances the adsorption uptake of AN, P, CP and NP onto GAC [58,71-72]. For example, the AN removal efficiency decreased from 97.8 to 89.5% as the AN concentration was increased from 20 to 200 mg dm^{-3} [58] and similar trends was found for removal of phenols [70,73]. The rate of removal of P and NP was faster initially and NP was more readily adsorbed than P, showing higher affinity of NP towards AC [70]. However, more P gets adsorbed than NP in the present study.

Adsorption dynamics

Two kinetic models, namely pseudo-first-order [74] and the pseudo-second-order model [41], were applied to the kinetic data in order to investigate the adsorption behavior of AN, P, CP and NP onto GAC

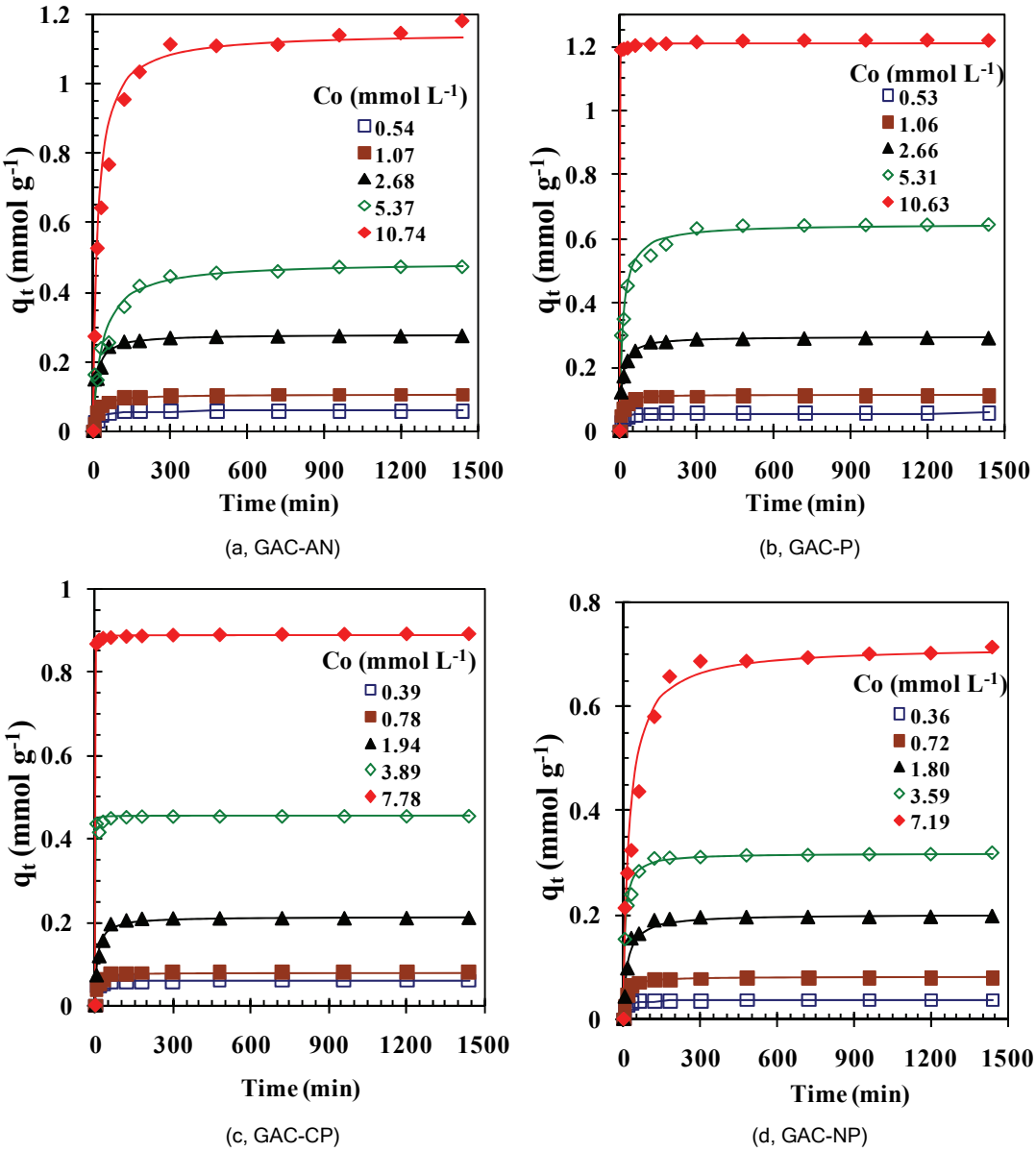

Figure 8. Effect of contact time on the adsorption of AN, P, CP and NP by GAC. Experimental data points given by the symbols and the lines predicted by the pseudo-second-order model. T = 303 K, m = 10 g dm^{-3}.

in the present study. The results of the fits of these models are given in Tables 2 and 3. The fits of experimental data to the pseudo first-order and the pseudo-second-order equations seemed to be quite good when correlation coefficients (R^2) obtained from non-linear regression analyses were examined. However, it was very difficult to decide which model represents the experimental data better solely on the basis of R^2. A better criterion to find the best model for the experimental data is the MPSD parameter. It is known that the lower the MPSD value, the better is the fit. When the MPSD values given in Tables 2 and 3 are examined, it can be seen that they are much smaller for the pseudo-second-order model as compared to that for the pseudo-first-order model, leading to the conclusion that the kinetic data of adsorption of AN, P, CP and NP onto GAC fit to the pseudo-second order model better than the pseudo-first-order model. Similar conclusions were made by various researchers [28,75-76] for removal of AN, 4-methylaniline, and 4-nitroaniline and CP onto various types of ACs.

Controlling mechanism

The overall adsorption process may be controlled either by one or more steps, *e.g.*, film or external diffusion, pore diffusion, surface diffusion and adsorption on the pore surface are the major steps involved during the adsorption process. Any one of these

Table 2. Kinetic parameters for the removal of AN and P by GAC. t = 24 h, C_0 = 0.54-10.74; 0.53-10.63 mmol dm^{-3}, m = 10 g dm^{-3}, T = 303 K

Parameter	AN-GAC adsorption system					P-GAC adsorption system				
	0.54	1.07	2.68	5.37	10.74	0.53	1.06	2.66	5.31	10.63
					Pseudo 1st order					
k_f / min^{-1}	0.046	0.047	0.065	0.026	0.043	0.121	0.068	0.060	0.052	0.779
$q_{e,cal}$ / mmol g^{-1}	0.059	0.105	0.259	0.444	1.111	0.057	0.111	0.288	0.639	1.211
$q_{e,exp}$ / mmol g^{-1}	0.0599	0.1057	0.235	0.472	0.275	0.058	0.112	0.291	0.645	1.216
R^2 (non-linear)	0.986	0.992	0.952	0.957	0.968	0.979	0.987	0.985	0.962	0.999
MPSD	26.94	15.79	43.18	58.38	43.54	22.49	23.14	26.87	42.04	2.82
					Pseudo 2nd order					
k_S / g $mmol^{-1}$ min^{-1}	1.98	0.55	0.28	0.06	0.05	2.85	1.36	0.33	0.12	8.46
h / mmol g^{-1} min^{-1}	0.007	0.006	0.022	0.014	0.0645	0.0096	0.0172	0.0287	0.0501	12.38
$q_{e,cal}$ / mmol g^{-1}	0.060	0.108	0.2780	0.4854	1.1487	0.0581	0.1123	0.2937	0.6496	1.21
R^2 (non-linear)	0.989	0.999	0.975	0.981	0.993	0.998	0.997	0.997	0.986	0.999
MPSD	17.16	12.29	24.13	38.13	19.13	5.74	7.53	10.18	21.82	2.41
					Weber Morris					
K_{id1} / mmol g^{-1} $min^{-1/2}$	0.006	0.008	0.016	0.027	0.059	0.005	0.007	0.025	0.014	0.001
I_1	0.012	0.017	0.099	0.057	0.304	0.018	0.043	0.274	0.129	1.195
R^2	0.916	0.875	0.896	0.936	0.998	0.953	0.893	0.901	0.923	0.958
K_{id2} / mmol g^{-1} $min^{-1/2}$	0.00008	0.0002	0.0002	0.0014	0.0032	0.00007	0.0002	0.0005	0.0002	0.0002
I_2	0.057	0.099	0.269	0.422	1.043	0.055	0.284	0.626	0.284	1.212
R^2	0.761	0.615	0.904	0.923	0.777	0.869	0.731	0.759	0.731	0.698

Table 3. Kinetic parameters for the removal of CP and NP by GAC. t = 24 h, C_0 = 0.39-7.78; 0.36-7.19 mmol dm^{-3}, m = 10 g dm^{-3}, T = 303 K

Parameter	CP-GAC adsorption system					NP-GAC adsorption system				
	0.39	0.78	1.94	3.89	7.78	0.36	0.72	1.80	3.59	7.19
					Pseudo 1st order					
k_f / min^{-1}	0.116	0.075	0.056	0.649	0.746	0.129	0.058	0.049	0.136	0.021
$q_{e,cal}$ / mmol g^{-1}	0.059	0.080	0.211	0.455	0.888	0.037	0.079	0.195	0.312	0.688
$q_{e,exp}$ / mmol g^{-1}	0.061	0.080	0.213	0.455	0.213	0.037	0.079	0.197	0.319	0.197
R^2 (non-linear)	0.942	0.983	0.995	0.996	0.999	0.989	0.996	0.995	0.967	0.982
MPSD	23.00	21.06	17.55	5.27	1.77	15.02	16.25	17.26	26.96	50.64
					Pseudo 2nd order					
k_S / g $mmol^{-1}$ min^{-1}	12.06	2.39	0.48	10.79	8.99	4.79	1.16	0.31	0.45	0.06
h / mmol g^{-1} min^{-1}	0.044	0.016	0.022	2.23	7.106	0.007	0.008	0.013	0.046	0.031
$q_{e,cal}$ / mmol g^{-1}	0.060	0.081	0.215	0.455	0.889	0.037	0.081	0.202	0.319	0.717
R^2 (non-linear)	0.994	0.994	0.997	0.997	0.999	0.999	0.998	0.993	0.996	0.985
MPSD	9.34	10.82	10.87	4.29	1.18	4.57	6.87	10.53	9.96	36.07
					Weber Morris					
K_{id1} / mmol g^{-1} $min^{-1/2}$	0.002	0.005	0.002	0.0046	0.0015	0.0003	0.0055	0.0114	0.0132	0.0409
I_1	0.043	0.036	0.043	0.408	0.869	0.013	0.023	0.071	0.170	0.117
R^2	0.984	0.862	0.984	0.712	0.773	0.876	0.829	0.814	0.963	0.996
K_{id2} / mmol g^{-1} $min^{-1/2}$	0.00004	0.00002	0.00007	0.00004	0.0002	0.00002	0.00009	0.0001	0.0003	0.001
I_2	0.059	0.079	0.209	0.454	0.886	0.036	0.076	0.193	0.306	0.661
R^2	0.969	0.836	0.841	0.943	0.987	0.890	0.773	0.741	0.919	0.912

steps, individually or in combination with other steps, may control the adsorption process. The characteristics of the adsorbate, adsorbent and the solution phase affect the adsorption process. The particle size of the adsorbent, concentration of the adsorbate, diffusion coefficient of the adsorbate in the bulk phase and the pores of the adsorbent, affinity towards adsorbent and degree of mixing are some of the impor-

tant factors. The external mass transfer controls the sorption process for the systems that have poor mixing, dilute concentration of adsorbate, small particle sizes of adsorbent and higher affinity of adsorbate for adsorbent. Film diffusion and adsorption on the pore surface are considered to be fast process [77] in a rapidly stirred batch adsorption process; whereas, intra-particle diffusion controls the adsorption process for a system with good mixing, large particle sizes of adsorbent, high concentration of adsorbate and low affinity of adsorbate for adsorbent [78].

In the present study, experiment were conducted at well-mixed condition of 150 rpm with AN, P, CP and NP concentration ranging from 0.54-10.74, 0.21--10.62, 0.15-7.78 and 0.14-7.19 mmol dm^{-3} to properly understand the controlling mechanism. In general, external mass transfer is characterized by the initial solute uptake [79] and can be calculated with the assumption that the uptake is linear for the first initial rapid phase (in the present study first 30 min). The initial adsorption rates (K_S in min^{-1}) were quantified as ($C_{30\ min}/C_0$)/30. For AN adsorption onto GAC, the calculated K_S values were found to be 0.00722, 0.0103, 0.01139, 0.0168 and 0.0185 min^{-1} for C_0 values of 0.54, 1.07, 2.68, 5.37 and 10.74 mmol dm^{-3}, respectively. For P adsorption onto GAC, the calculated K_S values were found to be 0.0069, 0.0076, 0.0096, 0.01028 and 0.00075 min^{-1} for C_0 values of 0.53, 1.06, 2.66, 5.31 and 10.63 mmol dm^{-3}, respectively. For CP adsorption onto GAC, the calculated K_S values were found to be 0.0038, 0.0072, 0.0089, 0.00357 and 0.00045 min^{-1} for C_0 values of 0.39, 0.78, 1.94, 3.89 and 7.78 mmol dm^{-3}, respectively. For NP adsorption onto GAC, the calculated K_S values were found to be 0.0040, 0.0067, 0.0075, 0.00908 and 0.01866 min^{-1} for C_0 values of 0.36, 0.72, 1.80, 3.59 and 7.19 mmol dm^{-3}, respectively.

Figures 9a-9d show the Weber and Morris [37] plot of q_t *versus* $t^{0.5}$ for all the adsorbates and the parametric values are given in Tables 2 and 3. If the plot of q_t *versus* $t^{0.5}$ satisfies the linear relationship with the experimental data, then the sorption process is supposed be controlled by intra-particle diffusion only. However, if the data exhibit multi-linear plots, then two or more steps influence the sorption process. The slope of the linear portions are defined as a rate parameters ($k_{id,1}$ and $k_{id,2}$) and are characteristics of the rate of adsorption in the region where intra-particle diffusion is rate controlling. In Figures 9a-9d, the data points are related by two straight lines. The curvature from the origin to the start of the first straight portion (not shown in figure) represents the boundary layer diffusion and/or external mass transfer effects [79-80]. The first straight portion depicts macro-pore diffusion and is attributed to the gradual equilibrium stage with intra-particle diffusion dominating. The second represents meso-pore diffusion and is the final equilibrium stage for which the intra-particle diffusion starts to slow down due to the extremely low adsorbate concentration left in the solution [80-81]. Extrapolation of the linear portions of the plots back to the *y*-axis gives the intercepts, which provide the measure of the boundary or film layer thickness. The deviation of straight lines from the origin indicates that the pore diffusion is not the sole rate-controlling step. Therefore, the adsorption proceeds *via* a complex mechanism [82] consisting of both surface adsorption and intra-particle transport within the pores of GAC. It can be inferred from the Figures 9a-9d that the diffusion of AN from the bulk phase to the external surface of GAC, which begins at the start of the adsorption process, is the fastest. It seems that the intra-particle diffusion of AN, P, CP and NP into meso-pores (second linear portion) is the rate-controlling step in the adsorption process. The portion of the plots are nearly parallel ($k_{id,2} \approx$ 0.00008–0.0032 mg g^{-1} $min^{-0.5}$, 0.00007--0.0032 mg g^{-1} $min^{-0.5}$, 0.00002–0.0002 mg g^{-1} $min^{-0.5}$, 0.00002–0.0013 mg g^{-1} $min^{-0.5}$), suggesting that the rate of adsorption AN, P, CP and NP into the meso-pores of GAC is comparable at all C_0. The slopes of the first portions ($k_{id,1}$) are higher for higher C_0 for AN, P, CP and NP, which corresponds to an enhanced diffusion of AN, P, CP and NP through macro-pores. This is due to the greater driving force at higher C_0.

The multi-phasic nature of intra-particle diffusion plot confirms the presence of both surface and pore diffusion. In order to predict the actual slow step involved, the kinetic data were further analyzed using Boyd kinetic expression. Equation (4) was used to calculate B_t values at different time t. The linearity of the plot of B_t *versus* time was used to distinguish whether surface and intra-particle transport controls the adsorption rate. It was observed that the relation between B_t and t (not shown here) was non-linear (R^2 range 0.828–0.991 for AN, 0.900–0.999 for P, 0.796--0.959 for CP and 0.764–0.994 for NP) at all concentrations, confirming that surface diffusion is the not the sole rate-limiting step. Thus, both surface and pore diffusion seem to be the rate-limiting step in the adsorption process and the adsorption proceeds via a complex mechanism.

The values of effective diffusion coefficient (D_e) were calculated from Eq. (5). Average values of D_e were found to be 2.24×10^{-10}, 2.43×10^{-10}, 3.65×10^{-10} and 2.89×10^{-10} m^2 s^{-1}, respectively, for the adsorption of AN, P, CP and NP onto GAC. This shows that CP

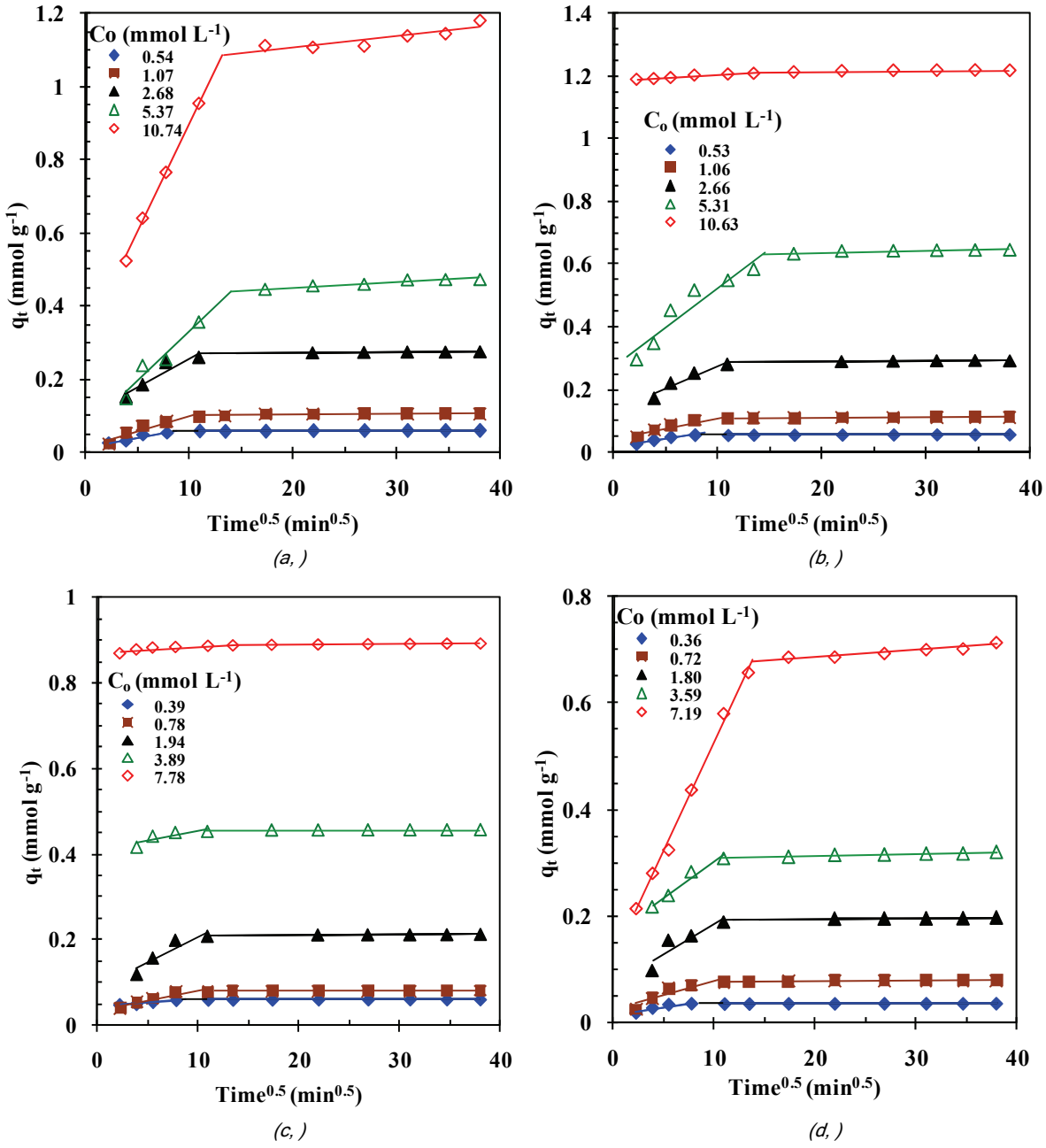

Figure 9. Weber and Morris intra-particle diffusion plot for the removal of AN, P, CP and NP by GAC. T = 303 K, m = 10 g dm^{-3}.

has a little higher overall pore diffusion rate. Similar average values of D_e (0.388×10^{-10}) were reported by Srivastava *et al.* [31] for adsorption of P onto AC.

Desorption study

Various solvents, viz. ethanol, HNO_3, HCl, NaOH, CH_3COOH, acetone and water were used in the present study for the elution of AN or P or CP or NP from the GAC [83]. AN or P or CP or NP-loaded GAC was stirred with 50 ml of various eluents and the results are shown in Figure 10. Among the various solvents, only NaOH was found to be a better elutant for the desorption of P, CP and NP with a maximum desorption efficiency of 5.43, 6.6 and 9.98%, respectively. HNO_3 was found to be a better elutant for the desorption of AN with a maximum desorption efficiency of 9.63%, respectively. Other solvents did not show any desorption efficiency. Negligible desorption efficiency by all solvents could be attributed to the chemical attachment between GAC and adsorbed AN, P, CP and NP, which prevented the adsorbed AN, P, CP and NP from being effectively desorbed by any solvent. NaOH was more removal efficiency compared to other solvents in the order of P, CP and NP,

due to stronger adsorbate-surface interactions with P, CP and NP [75]. Subsequent thermal regeneration was needed to remove additional adsorbates.

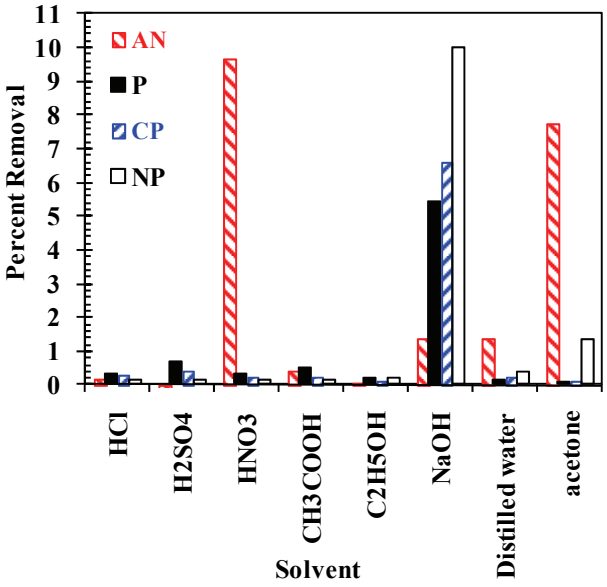

Figure 10. Desorption efficiencies of AN, P, CP and NP by various desorbing agents. T =3 03 K, t = 24 h, C_0 (desorbing agents) = 0.1 N, m = 1 g dm^{-3}.

Spent-GAC was thermal desorbed by process described in material and method section. Thermally desorbed GAC was again used for adsorption. This cycle of adsorption-desorption was repeated five times. Percent removal of AN, P, CP and NP in those cycles is shown in Figure 11. It is seen that the spent-adsorbent can be reused for a number of adsorption-desorption cycles. Percent removal of AN, P, CP and NP, however, decreased after each adsorption-desorption cycle.

It is necessary to properly dispose of the spent GAC and/or utilize it for some beneficial purpose if possible. The dried spent-GAC can be used directly or by making fire-briquettes in the furnace combustors/incinerators to recover its energy value. AN, P, CP and NP loaded adsorbents were studied for their thermal degradation characteristics by thermo gravimetric instrument. The thermogravimetric analysis (TGA), differential thermal analysis (DTA) and differential thermal gravimetery (DTG) curves of the blank, and AN-, P-, CP-and NP-loaded GAC at the heating rate of 10 K/min are shown in Figures 12a-12c. The TG traces show the loss of moisture and the evolution of some light weight molecules including water upto 500 °C. The weight loss was 18% for blank-GAC, 10.2% for AN-GAC, 13.7% for P-GAC, 14% for CP-GAC and 22.9% for NP-GAC. Higher temperature drying (>100 °C) occurs due to loss of the surface tension bound water of the particles. Blank, AN, P, CP-and NP-GAC do not show any endothermic transition between room temperature and 400 °C, indicating the lack of any crystalline or other phase change during the heating process [84]. The rate of weight loss was found to increase between 500 and 601 °C (81% weight loss), 501 and 701 °C (67.2%), 499 and 601 °C (79.3%), 500 and 599 °C (78.5%) and 500 and 600 °C (49.4%) for blank, AN, P, CP and NP-GAC, respectively. In these temperature ranges, the AN, P, CP and NP-loaded GAC oxidize and completely lose their weight. The strong exothermic peak centered between 500-660 °C is due to the oxidative degradation of the samples. This broad peak as that observed from the first derivative loss curve (DTG) may be due to the combustion of carbon species. TGA and DTA curves could be used to deduce drying and thermal degradation characteristics. Blank GAC has a heating value of about 8.26 MJ/kg. Thus, the GAC along-with the adsorbed AN, P, CP and NP can be dried and used as a fuel in the boilers/incinerators, or can be used for the production of fuel-briquettes. The bottom ash may be blended with clay to make fire bricks, or with cement-concrete mixture to make colored building blocks thus disposing of AN, P, CP and NP through chemical and physical fixation. Thus, spent GAC could not only be safely disposed of, but also its energy value can be recovered.

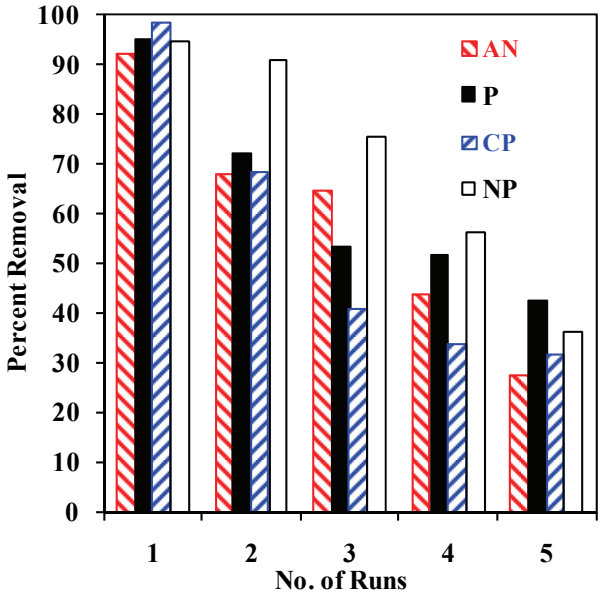

Figure 11. Thermal desorption efficiencies of AN, P, CP and NP in a sequence of adsorption/desorption cycle.

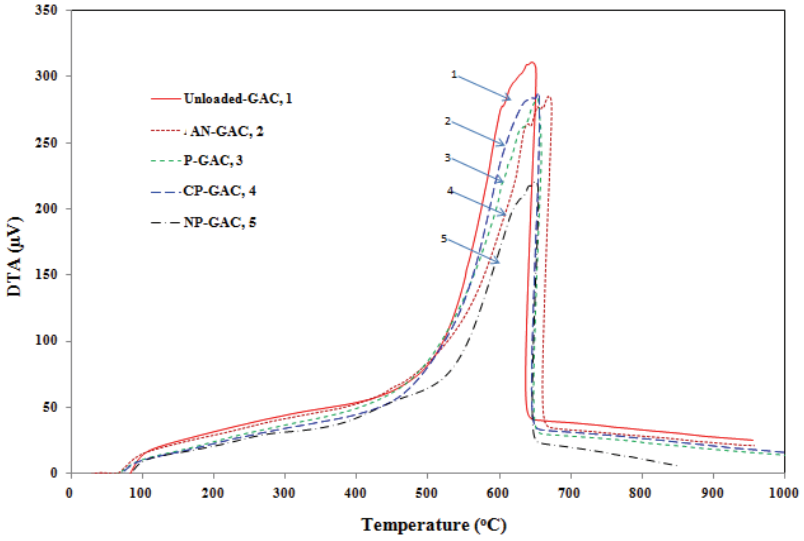

(a)

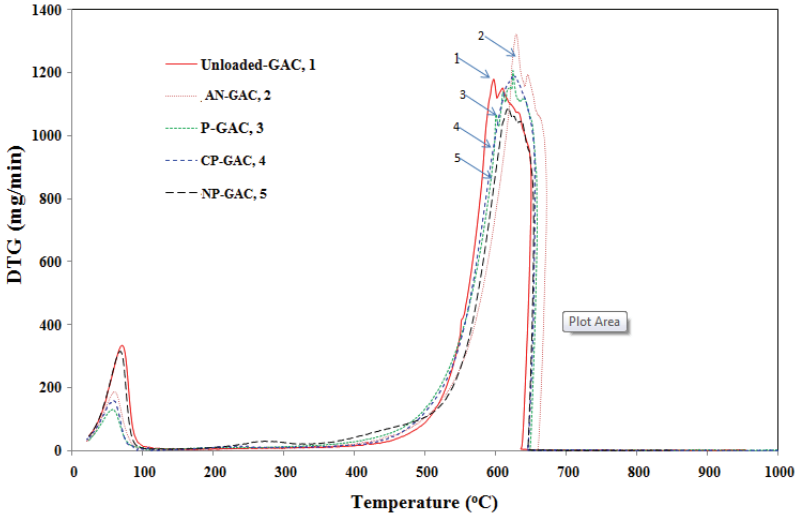

(b)

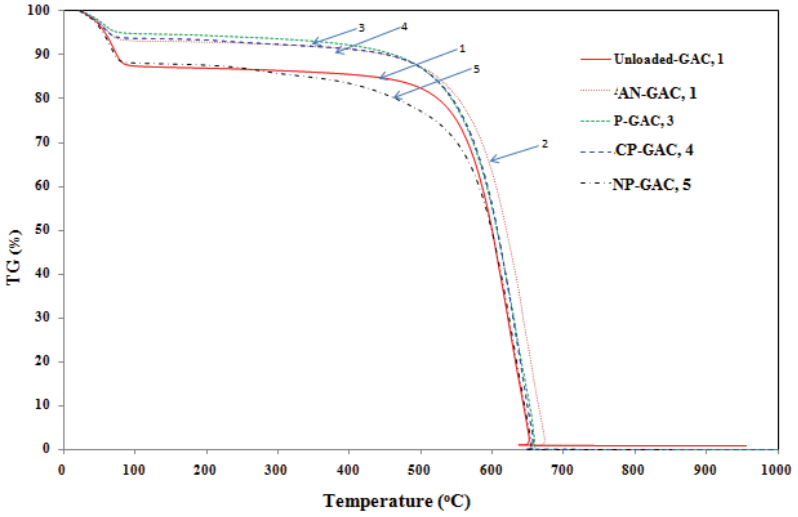

(c)

Figure 12. DTA (a), DTG (b) and %TG (c) graphs of virgin and AN, P, CP and NP loaded GAC under oxidizing atmosphere.

CONCLUSION

The present study shows that the GAC is an effective adsorbent for the removal of AN, P, CP and NP from aqueous solutions. The amount of AN, P, CP and NP uptake (mmol g^{-1}) was found to increase with an increase in AN, P, CP and NP concentration and contact time. Equilibrium between the AN, P, CP and NP in the solution and on the GAC surface was practically achieved in 5 h. The sorption kinetics followed a pseudo second-order model. AN, P, CP and NP loaded GAC regeneration was studied using various solvents as well as by heating the spent GAC at 623 K. Solvent aided regeneration of GAC was found to be very less with maximum desorption efficiency of 9.63, 5.43, 6.6 and 9.98%, respectively, shown by AN-, P-, CP-and NP-GAC system. Thermal desorption of GAC worked well for at least five adsorption-desorption cycle, with continuous decrease in adsorption efficiency after each cycle. Spent-GAC can be used as co-fuel in boiler-furnaces/incinerators.

REFERENCES

[1] Q-S Liu, T. Zheng, P. Wang, J-P Jiang, N. Li, Chem. Eng. J. **157** (2010) 348

[2] C.M. Castilla, Carbon **42** (2004) 83-94

[3] K. Laszlo, E. Tombacz, C. Novak, Colloids Surfaces, A **306** (2007) 95-101

[4] K. Zheng, B.C. Pan, Q.J. Zhang, Sep. Purif. Technol. **57** (2007), 250-256

[5] B. Nasr, M.F. Ahmadi, A. Gadri, Canadian J. Civil Eng. **36** (2009) 683-689

[6] F.S.H. Abram, I.R. Sims, Water Res. **16** (1982) 1309--1312

[7] N.B. Ress, K.L. Witt, J. Xu, J.K. Haseman, J.R. Bucher, Mutat. Res. Gen. Toxicol. Environ. Mutagen. **521** (2002) 201-208

[8] M.F. Khan, P.J. Boor, B.S. Kaphalia, N.W. Alcock, G.A. S. Ansari, Fund. Appl. Toxicol. **25** (1995) 224-232

[9] S. Hussain. J. Chromatogr. **18** (1965) 419

[10] P. Patnaik, A Comprehensive Guide to the Hazardous Properties of Chemical Substances, 2nd ed., New York, John Wiley and Sons, 1999

[11] L.H. Keith, W.A. Telliard. Environ. Sci. Technol. **13** (1979) 416

[12] USEPA, Federal Register, Vol. 52, No. 131, USEPA, Washington DC, 1987, p. 25861

[13] S.H. Gheewala, A.P. Annachhatre, Water Sci. Technol. **36** (1997) 53-63

[14] F.J. O'Neill, K.C.A. Bromley-Challenor, R.J. Greenwood, J.S. Knapp, Water Res. **34** (2000) 4397-4409

[15] J.J. Barbier, L. Oliviero, B. Renard, D. Duprez, Catal. Today **75** (2002) 29-34

[16] S.R. Jadhav, N. Verma, A. Sharma, P.K. Bhattacharya, Sep. Purif. Technol. **24** (2001) 541-557

[17] F. Pithan, C. Staudt-Bickel, R.N. Lichtenthaler, Desalination **148** (2002) 1-4

[18] Y. Jiang, C. Petrier, T.D. Waite, Ultrason. Sonochem. **9** (2002) 163-168

[19] X. H. Qi, Y.Y. Zhuang, Y.C. Yuan, W.X. Gu, J. Hazard. Mater. **90** (2002) 51-62

[20] E. Brillas, J. Casado, Chemosphere **47** (2002) 241-248

[21] P.X. Wu, Z.W. Liao, H.F. Zhang, J.G. Guo, Environ. Int. **26** (2001) 401-407

[22] T.A. Ozbelge, O.H. Ozbeze, S.Z. Baskaya, Chem. Eng. Process **41** (2002) 719

[23] K. Karim, S.K. Gupta, Biores. Technol. **80** (2001) 179-186

[24] V. Kavita, K. Palanivelu, Chemosphere **55** (2004) 1235--1243

[25] S. Ghasempur, S.F. Torabi, S.O. Ranaei-siadat, M. Jalali-Heravi, N. Ghaemi, K. Khajeh, Environ. Sci. Technol. **41** (2007) 7073-7079

[26] J. Yan, R. Nanqi, C. Xun , W. Di, Q. Liyan, L. Sen, Chinese J. Chem. Eng. **16** (2008) 796-800

[27] F. Orshansky, N. Narkis, Water Res. **31** (1997) 391-398

[28] L.M. Cotoruelo, M.D. Marqus, J. Rodrguez-Mirasol, T. Cordero, J.J. Rodrguez, Ind. Eng. Chem. Res. **46** (2007) 2853-2860

[29] A. Bhandari, I. Cho, Proceedings of the 1999 conference on Hazardous Waste Research, 1999, pp. 27-40

[30] A.A. Daifullah, B.S. Girgis, Water Res. **32** (1998) 1169--1177

[31] V.C. Srivastava, M.M. Swamy, I.D. Mall, B. Prasad, I.M. Mishra, Colloid Surfaces, A **272** (2006) 89-104

[32] J.S.M. Zogorski, S.D. Faust, J.H. Haas Jr., J. Colloid Interf. Sci. **55** (1976) 329-341

[33] I.I. Salame, T.J. Bandosz, J. Colloid Interface Sci. **264** (2003) 307-312

[34] T.E.M. Ten Hulscher, G. Cornelissen, Chemosphere **32** (1996) 609-626

[35] A.R. Khan, T.A. Al-Bahri, A. Al-Haddad, Water Res. **31** (1997) 2102-2112

[36] S. Suresh, V. C Srivastava, I. M. Mishra, J. Chem. Eng. Data. **56** (2011) 811-818.

[37] W.J. Weber Jr., J.C. Morris, J. Sanitary Eng. Div. Proceed. Am. Soc. Civil. Eng. **89** (1963), 31-59

[38] E. Boyd, A.W. Adamson, L.S. Meyers, J. Am. Chem. Soc. **69** (1947) 2836-2848

[39] A.H.P. Skelland, Diffusional Mass Transfer. Wiley, NY, 1974

[40] T. Vermeulen, Ind. Eng. Chem. **45** (1953) 1664-1670

[41] Y.S. Ho, G. McKay, Process Biochem. **34** (1999) 451-465

[42] D.W. Marquardt, J. Soc. Ind. Appl. Math. **11** (1963) 431--441

[43] M. Ibrahim, E. Koglin, Acta Chim. Siov. **52** (2005) 159--163

[44] A.G. Galinos, T.F. Zafiropoulos **109** (1978) 1475-1479

[45] I. Poljansek, M. Krajnc, Acta chim. slov. **52** (2005) 238--244

[46] B. Bardakci, J. Arts Sci. 7 (2007) 13-19

[47] M. Paku, A. Swiatkowski, M. Walczyk, S. Biniak, Colloid Surf. A: Physicochem. Eng. Aspects, **260** (2005) 145-155

[48] W. Zierkiewicz, D. Michalska, T. Zeegers-Huyskens, J. Phys. Chem., A **104** (2000) 11685-11692

[49] B. Pandit, U. Chudasama, Bull. Mater. Sci. **24** (2001) 265-271

[50] M. Ahmaruzzaman, S.L. Gayatri, Chem. Eng. J. **158** (2010) 173-180

[51] C.A. Leon y Leon, J.M. Solar, V. Calemma, L.R. Radovic, Carbon **30** (1992) 797-811

[52] A. Contescu, M. Vass, C. Contescu, K. Putyera, J.A. Schwarz, Carbon **36** (1998) 247-258

[53] C. Moreno-Castilla, J. Rivera-Utrilla, J.P. Joly, M.V. Lopez-Ramon, M.A. Ferro-Garcia, F. Carrasco-Martin, Carbon **33** (1995) 1417-1423

[54] F. Villacanas, M.F.R. Pereira, J.J.M. Orfao, J.L. Figueiredo, J. Colloid Interface Sci. **293** (2006) 128-136

[55] D. Tang, Z. Zheng, K.L.J. Luan, J. Zhang. J. Hazard. Mater. **143** (2007) 49-56

[56] K. Yang, W. Wu, Q. Jing, L. Zhu, Environ. Sci. Technol. **42** (2008) 7931-7936

[57] S. Fiore, M.C. Zanetti, Am. J. Environ. Sci. **5** (2009) 546--554

[58] H. Zheng, D. Liu, Y. Zheng, S. Liang, Z. Liu, J. Hazard. Mater. **167** (2009) 141

[59] R.W. Coughlin, F.S. Ezra, Environ. Sci. Technol. **2** (1968) 291-297

[60] M. Franz, H.A. Arafat, N.G. Pinto, Carbon **38** (2000) 1807-1819

[61] J. Mattson, H. Mark, M. Malbin, J. Weber, W.J. Crittenden, J. Colloid Interf. Sci. **31** (1969) 116-130

[62] A. Star, T.R. Han, J-C.P. Gabriel, K. Bradley, G. Gruner, Nano Lett. **3** (2003) 1421-1423

[63] C. Hansch, A. Leo, R.W. Taft, Chem. Rev. **91** (1991) 165--195

[64] D. Lin, B. Xing, Environ. Sci. Technol. **42** (2008) 7254-7259

[65] D.A. Blanco-Martinez, L. Giraldo, J.C. Moreno-Pirajan, J. Hazard. Mater.**169** (2009) 291-296

[66] W. Chen, L. Duan, D.Q. Zhu, Environ. Sci. Technol. **41** (2007) 8295-8300

[67] K. Shakir, H.F. Ghoneimy, A.F. Elkafrawy, S.G. Beheir, M. Refaat, J. Hazard. Mater. **150** (2008) 765-773

[68] S.M. Bilgili, J. Hazard. Mater. **B137** (2006) 157-164

[69] H. Zheng, Y. Wang, Y. Zheng, H. Zhang, S. Liang, M. Long, Chem. Eng. J. **143** (2008) 117-123

[70] A. Kumar, S. Kumar, S. Kumar, D.V. Gupta, J. Hazard. Mater. **147** (2007) 155-166

[71] F. Akbal, J. Environ. Manage. **74** (2005) 239-244

[72] Y-C. Chen, P-J. Tsai, A-L. Mou, Environ. Sci. Technol. **43** (2009) 4459-4465

[73] F.A. Banat, B. Al-Bashir, S. Al-Asheh, O. Hayajneh, Environ. Poll. **107** (2000) 391-398

[74] S. Langergren, B.K. Svenska, Veternskapsakad Handlinger **24** (1898) 1-39

[75] C. Jianguo, L. Aimin, S. Hongyan, F. Zhenghao, L. Chao, Z. Quanxing. J. Hazard. Mater. **B124** (2005) 173-180

[76] B.H. Hameed, L.H. China, S. Rengaraj, Desalination **225** (2008) 185-198

[77] W.J. Weber Jr., in: Physicochemical processes for water quality control, Wiley-Interscience, New York, 1972, p. 211

[78] R. Aravindhan, J.R. Rao, B.U. Nair, J. Hazard. Mater. **142** (2007) 68-76

[79] G. McKay, S.J. Allen, I.F. McConvey, M.S. Otterburn, J. Colloid Interface Sci. **80** (1981) 323-339

[80] J. Crank, The mathematics of diffusion, 84, first ed., Oxford Clarendon Press, London, 1965

[81] D. Reichenberg, J. Am. Chem. Soc. **75** (1953) 587-589

[82] A.K. Chaturvedi, K.C. Pathak, V.N. Singh, Appl. Clay Sci. **3** (1988) 337-346

[83] I.D. Mall, V.C. Srivastava, G.V.A. Kumar, I.M. Mishra, Colloids Surfaces, A **278** (2006) 175-187

[84] W. Ng, H. Cheung, G. McKay, J. Colloid Interf. Sci. **255** (2002) 64-74.

S. SURESH[1]
V.C. SRIVASTAVA[2]
I.M. MISHRA[2]

[1]Department of Chemical Engineering, Maulana Azad National Institute of Technology Bhopal, Bhopal, India
[2]Department of Chemical Engineering, Indian Institute of Technology Roorkee, Roorkee, India

NAUČNI RAD

PROUČAVANJE KINETIKE ADSORPCIJE I REGENERACIJE ANILINA, FENOLA, 4-HLORFENOLA I 4-NITROFENOLA POMOĆU AKTIVNOG UGLJA

U ovom radu je predstavljena kinetička studija adsorpcije anilina (AN), fenola (P), 4-hlorofenola (CP) i 4-nitrofenola (NP) iz vodenog rastvora na granule aktivnog uglja (GAC). FTIR spektralna analiza pokazuje da se transmitanca pikova povećava nakon punjenja sa AN, P, CP i NP, ukazujući na značajno učešće ovih funkcionalnih grupa u adsorpciji, koja je u ovom slučaju hemisorptivne prirode. Brzina rekcija adsorpcije predstavlja reakciju pseudo drugog reda i dinamika adsorpcije AN, P, CP i NP je kontrolisana kako od strane površine pora tako i od difuzije. Koeficijent difuzije je reda veličine 10^{10} $m^2 \cdot s^{-1}$. Utvrđeno je da je termalna desorpcija na 623 K daleko efikasnija od desorpcije rastvaračem. GAC se vrši sa najmanje pet adsorpciono-desorpcionih ciklusa, uz stalno smanjenje efikasnosti adsorpcije nakon svake termičke desorpcije. Zahvaljujući relativno visokoj vrednosti zagrevanja, GAC može se koristiti kao dodatno gorivo u proizvodnji toplote za bojlere i peći.

Ključne reči: anilin, fenoli, kinetika, pseudo prvi red, pseudo drugi red, desorpcija, rastvarač, termalni.